

**Magnetization-dependent Rashba splitting of quantum well states at the Co/W interface**P. Moras,<sup>1</sup> G. Bihlmayer,<sup>2</sup> P. M. Sheverdyaeva,<sup>1</sup> S. K. Mahatha,<sup>1</sup> M. Papagno,<sup>1,3</sup> J. Sánchez-Barriga,<sup>4</sup>  
O. Rader,<sup>4</sup> L. Novinec,<sup>5</sup> S. Gardonio,<sup>5</sup> and C. Carbone<sup>1</sup><sup>1</sup>*Istituto di Struttura della Materia, Consiglio Nazionale delle Ricerche, 34149 Trieste, Italy*<sup>2</sup>*Peter Grünberg Institut and Institute for Advanced Simulation, Forschungszentrum Jülich and JARA, 52425 Jülich, Germany*<sup>3</sup>*Dipartimento di Fisica, Università della Calabria, 87036 Arcavacata di Rende (Cs), Italy*<sup>4</sup>*Helmholtz-Zentrum Berlin für Materialien und Energie, Elektronenspeicherring BESSY II, Albert-Einstein-Straße 15, 12489 Berlin, Germany*<sup>5</sup>*Materials Research Laboratory, University of Nova Gorica, Vipavska 13, 5000 Nova Gorica, Slovenia*

(Received 12 November 2014; revised manuscript received 17 April 2015; published 11 May 2015)

Exchange and Rashba spin-orbit interactions are expected to couple at ferromagnetic-metal/heavy-metal interfaces and influence their electronic structure. We examine these largely unexplored effects in Co(0001) films on W(110) by angle-resolved photoemission spectroscopy. We find breaking of inversion symmetry in the band dispersion of magnetic quantum well states along structurally equivalent directions of the Co films. *Ab initio* calculations ascribe this unusual band behavior to the relative orientation of coexisting exchange and Rashba fields. These findings elucidate fundamental interface electronic effects, which are associated to spin-orbit phenomena at ferromagnetic-metal/heavy-metal junctions.

DOI: [10.1103/PhysRevB.91.195410](https://doi.org/10.1103/PhysRevB.91.195410)

PACS number(s): 73.21.Fg, 75.70.Tj, 75.30.Et

**I. INTRODUCTION**

Spintronics is the branch of electronics that aims at studying and manipulating the spins of solids, especially in the perspective of exploiting novel spin-based functionalities in electronic devices. One of the most promising discoveries in this field is the current-induced magnetization switching occurring in ferromagnetic-metal (FM)/heavy-metal (HM) bilayers [1–5]. This phenomenon is currently interpreted according to two different models, with common origin in the spin-orbit interaction (SOI), based on either the spin Hall effect [2,6] or the Rashba effect [3,7–9]. However, both models appear not to be adequate to provide a comprehensive description of the phenomenon [4]. In fact, realistic calculations of the spin-orbit torques acting on the FM layer would require a detailed knowledge of the electronic structure of the systems, which is not available so far. In the present paper we analyze a model FM/HM junction, where finite size effects in the FM layer give experimental access to the electronic properties of the buried interface [10,11]. Our study points out unusual magnetization-dependent features in the ground-state electronic structure of the system. These effects are found to derive from the combination of a high exchange interaction and high Rashba SOI, which characterize the FM and HM materials of the heterostructure.

The effects of the Rashba SOI on the electronic states of solid systems are well documented. The surface bands of several heavy element materials show Rashba-derived spin splittings, observable by angle-resolved photoemission investigations. The first experimentally identified case was the Shockley surface state of Au(111), which displayed spin-up and spin-down parabolic bands shifted to opposite  $k_{\parallel}$  values with respect to the  $\bar{\Gamma}$  point [12]. Large Rashba splittings were identified in surface alloys [13] and surface superstructures [14,15], as well as on the surfaces of topological insulators [16]. An intriguing situation was encountered in thick Gd(0001) [17] and Tb(0001) [18] films and their surface oxides. The spin-polarized *sd*-like surface states of these systems display an asymmetric band dispersion with respect

to  $\bar{\Gamma}$  that reverses upon switching the film magnetization. The experimental observations are ascribed to a combination of the exchange and Rashba effects.

Similarly to surfaces, interfaces lack full translational symmetry and give, like these, rise to the Rashba effect. Several experimental works pointed out the strength of the interface Rashba SOI in thin noble and simple metal films on HM substrates. Spin- and angle-resolved photoemission analyses of Cu [19], Ag [20], Au [19,20], and Al [21] monolayers on W(110) highlighted in a direct way the formation of Rashba-split interface states. In thicker films the interface Rashba SOI has less obvious electronic structure effects. Surface and interface act on the valence electrons of a metal film as confining potential walls, giving rise to a set of discrete quantum well (QW) states, in close analogy with the particle-in-a-box picture [Fig. 1(a)]. These two-dimensional standing waves, extended in the whole film thickness, are effective, though indirect, probes of interface interactions [10,11], which influence their energy-momentum band dispersion [Fig. 1(b)]. Indeed, spin-dependent gap openings were observed by photoemission along the QW bands of Al [21] and Au [22] films on W(110) and ascribed to the large spin-orbit coupling of the substrate.

In this paper we analyze the electronic structure of ferromagnetic Co(0001) films, supporting the formation of discrete and spin-polarized *d*-electronic bands near the Fermi level ( $E_F$ ), grown on W(110), characterized by a large spin-orbit coupling. Angle-resolved photoemission highlights strong asymmetries in the energy-momentum dispersion of the Co QW states, which reverse upon switching the film magnetization. We show that this unusual band behavior is not observed in Co films on Mo(110), which are isostructural to the Co/W system but with reduced SOI. *Ab initio* electronic structure calculations link the experimental findings with the presence of a strong interface Rashba field, induced by the broken inversion symmetry in the vicinity of the heavy W substrate. Depending on the in-plane momentum, a component of this Rashba field is added to the exchange field, leading to the observed dependence of the QW band dispersions on

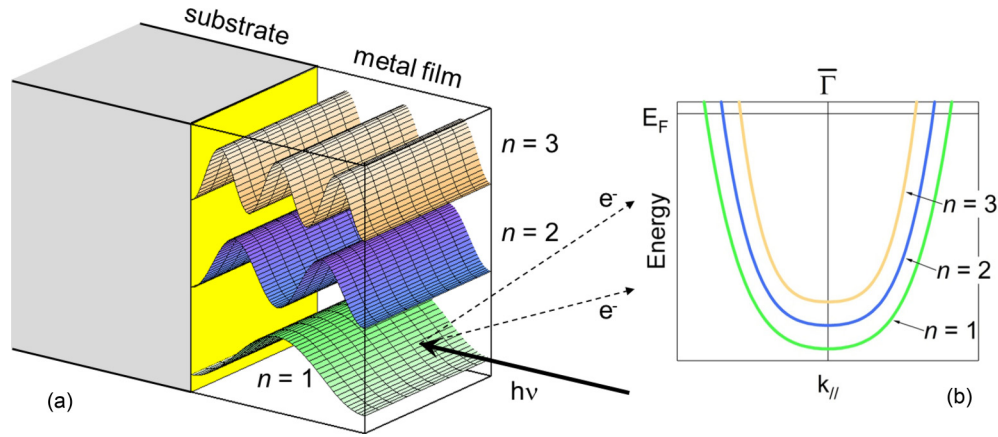


FIG. 1. (Color online) (a) Surface (transparent) and interface (yellow) planes act as potential walls for the film valence electrons. The confined geometry gives rise to a set of two-dimensional standing waves, called QW states, that extend in the whole film thickness. These states can be labeled with the main quantum number  $n$ , i.e., the number of maxima of the respective charge densities along the direction of confinement. (b) The extended spatial character of the QW-state wave functions makes their energy-momentum band dispersion, observable by angle-resolved photoemission spectroscopy, an indirect probe of interface interactions.

the magnetization direction. This model system allows thus to directly highlight fundamental magnetization-dependent electronic effects occurring at the interface between HM and FM materials.

II. METHODS

The experiments were carried out at the VUV-Photoemission beamline at Elettra (Trieste) and at the ARPES  $1^2$  end station at BESSY II (Berlin). The W(110) crystal was prepared by repeated high temperature flash-annealing cycles in oxygen atmosphere until a sharp  $1 \times 1$  low-energy electron diffraction (LEED) pattern and well-resolved W  $4f$  surface core level component were observed. Co(0001) films grow on W(110) in the Nishiyama-Wassermann orientation [23]. Figure 2(a) reports surface Brillouin zones and symmetry axes of the two materials and defines  $k_x$  and  $k_y$  to be parallel to the  $[11\bar{2}0]$  and  $[1\bar{1}00]$  surface axes of Co(0001), respectively. Cobalt was deposited at room temperature from an electron-bombarded rod. The LEED showed a  $1 \times 1$  hexagonal pattern with blurred spots, with respect to those of clean W(110). After annealing to 150 °C the films displayed much sharper diffraction spots and a QW-state band pattern in the photoemission signal near  $E_F$ . Photoemission spectra of Co films [Figs. 2(b)–2(d)] display several QW bands crossing  $E_F$ , which increase in number as the film thickness increases. The direct observation of these QW states allowed precise

definition of the film thickness in terms of Co monolayers (MLs). The films were uniformly and remanently magnetized by passing high-current pulses through a coil placed near the sample. Within the investigated thickness range (6–24 Co ML) the films were found to be in-plane magnetized along the Co  $[1\bar{1}00]$  surface direction by magnetic linear dichroism measurements of the Co  $3p$  core levels (see Fig. 1S of the Supplemental Material [24]). The magnetization ( $\mathbf{M}$ ) and light polarization dependence of the valence-band photoemission spectra were investigated with 56 eV photons, where the effects of size quantization in the Co films were best observed. The same procedures were followed to grow and analyze Co films on Mo(110).

Density functional theory (DFT) calculations for free-standing Co(0001) films and Co/W junctions were performed using the full-potential linearized augmented plane wave method in thin film geometry [25] as implemented in the FLEUR code [26]. We used the generalized gradient approximation to the exchange correlation potential [27] and, where indicated, the effects of SOI were included in the Hamiltonian in a nonperturbative scheme [28]. In the calculation, we have to deal with the lattice mismatch between hcp Co(0001) and bcc W(110). Since we are interested in the Co QW states, we choose to keep the hexagonal Co in-plane lattice constant fixed and relax all layers of the Co/W junctions along the  $z$  (out-of-plane) direction. We compared the results to calculations where the centered rectangular in-plane unit

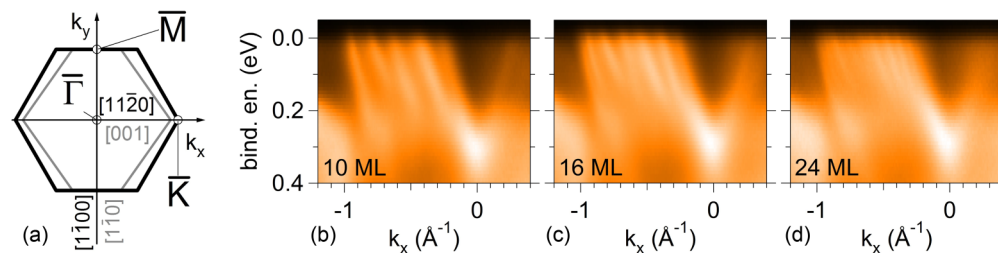


FIG. 2. (Color online) (a) Surface Brillouin zones and high-symmetry directions of Co(0001) (black line) and W(110) (gray line). (b–d) Photoemission spectra acquired along  $k_y = 0$ , corresponding to the Co  $[11\bar{2}0]$  axis, for Co films of different thickness. The light is  $p$  polarized.

cell of the W(110) surface was used and found qualitatively similar results.

### III. RESULTS AND DISCUSSION

Figure 3(a) shows a constant energy cut of the photoemission signal near  $E_F$  for the 10-ML Co film on W(110). The data were acquired according to the procedure described in the Supplemental Material [24], which avoids asymmetries that vary with the light incidence angle. In Fig. 3(a) the sample magnetization is set to point along the positive  $k_y$  direction. The QW states present an oval shape near  $\bar{\Gamma}$  and more complex constant energy contours, characterized by multiple breaks, at larger in-plane momenta. At a closer look, the image shows, despite the chosen symmetric geometry, left-right asymmetries, which disappear only very near to the vertical axis. These effects can be easily visualized in the photoemission spectra acquired along  $k_y = 0$  [Fig. 3(b)]. The QW states enclosed in rectangular boxes display asymmetric energy-momentum dispersions with respect to  $\bar{\Gamma}$ , as highlighted by the different momentum distribution curves at  $E_F$  (white lines). The QW-state crossing  $E_F$  at  $k_x = -0.65 \text{ \AA}^{-1}$ ,

for instance, has its counterpart at  $k_x = 0.60 \text{ \AA}^{-1}$  on the right-hand side of the figure. Smaller band shifts (in the order of  $0.02 \text{ \AA}^{-1}$ ) are also found by comparing the dispersion of other QW states near  $\bar{\Gamma}$  along opposite  $k_x$  directions. Instead, the photoemission spectra recorded along  $k_x = 0$ , i.e., along the magnetization direction [Fig. 3(c)], show fully symmetric bands.

The observed asymmetries could arise from magnetic dichroism effects [29–31] (leading to intensity differences in the spectra when the magnetization is reversed) or from magnetization-dependent ground-state properties of the Co/W junction. To ascertain their origin, we examined the electronic states of Co films on Mo(110), which are isostructural to Co films on W(110) and magnetized, likewise, along the Co  $[1\bar{1}00]$  surface direction [32,33]. Mo ( $Z = 42$ ) is much lighter than W ( $Z = 74$ ) and has largely reduced spin-orbit effects [20]. The QW-state contours for a 10-ML Co film on Mo(110) define on a constant energy plane a symmetric pattern with respect to the vertical axis [Fig. 3(d)]. The photoemission spectra measured along  $k_y = 0$  [Fig. 3(e)] reveal only small intensity differences of QW peaks at opposite  $k_x$  values, which derive from magnetic linear dichroism effects. At variance with

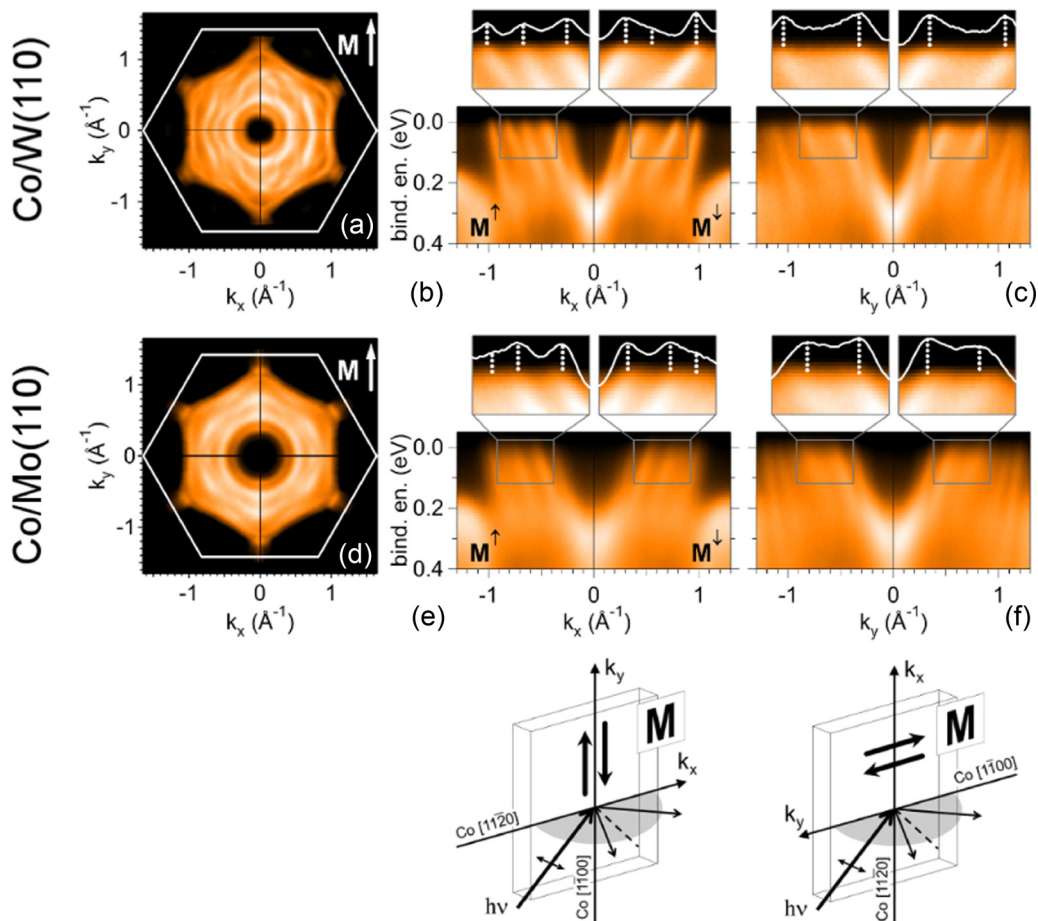


FIG. 3. (Color online) Photoemission data for (upper row) 10 ML Co on W(110) and (lower row) 10 ML Co on Mo(110). Light is p polarized. (a,d) Constant energy cuts at 50 meV below  $E_F$ , with an energy integration of  $\pm 25$  meV. (b,e) Spectra measured along the  $k_y = 0$  axis, with opposite magnetization (perpendicular to the scattering plane of the experiment) in the geometry sketched below the two panels. Energy distribution curves at  $E_F$  (white lines) point out the different (asymmetric vs symmetric) QW band behavior in Co/W and Co/Mo. (c,f) Spectra measured along the  $k_x = 0$  axis, i.e., with the magnetization in the scattering plane of the experiment in the geometry sketched below the two panels. In both cases no asymmetries are observed.

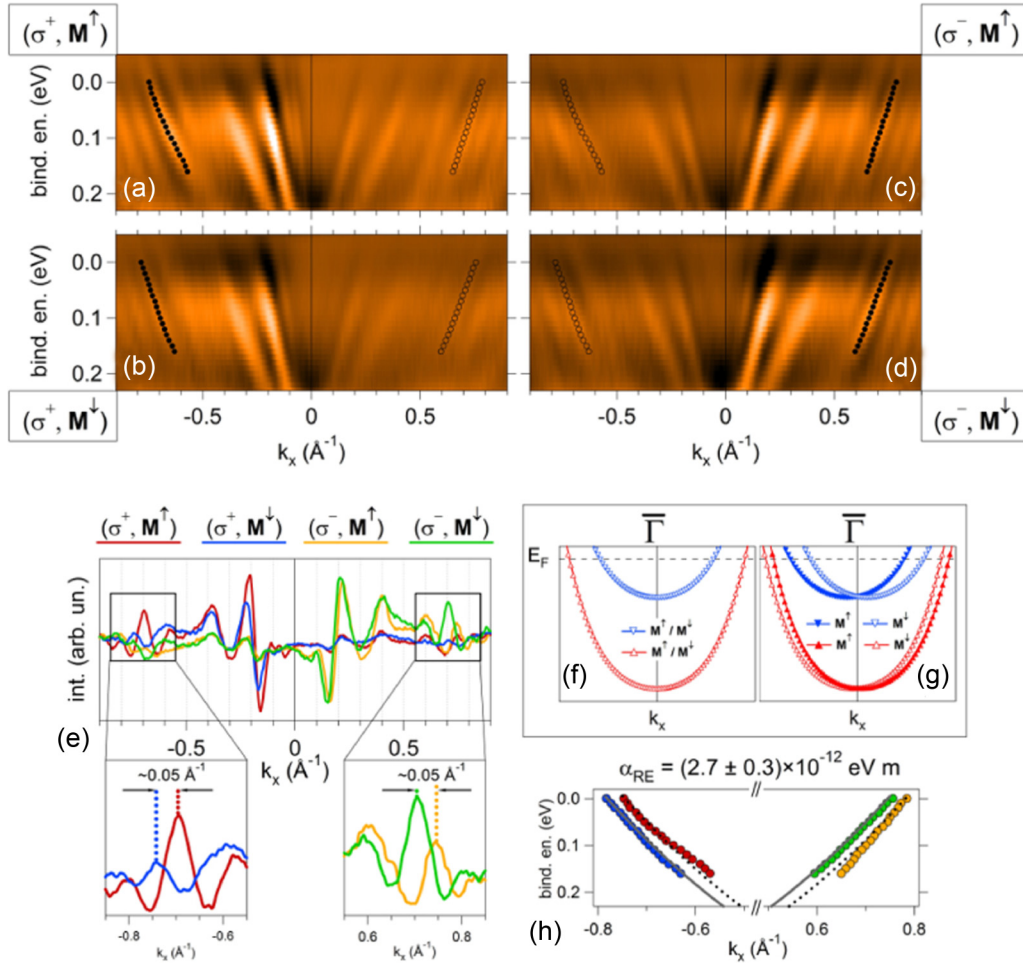


FIG. 4. (Color online) (a–d) Second derivative photoemission spectra of 14 ML Co on W(110) for the four possible combinations of light polarization and sample magnetization. Panels (a) and (d), as well as (b) and (c), look like mirror symmetric images with respect to  $k_x = 0$ . Black dots highlight the dispersion of the QW state displaying the largest magnetization-dependent band asymmetry. (e) Momentum distribution curves extracted from panels (a–d) at 50-meV binding energy. The close-up areas highlight the  $k_x$  shifts observed upon switching the sample magnetization. (f) Schematic band diagram of exchange-split electronic states. Their dispersion does not depend on the direction of magnetization. (g) Same as (f) for a system subject to the Rashba interaction, like Co films on W(110). The band dispersion depends on the magnetization. The Rashba-exchange constant  $\alpha_{RE}$  is different for the opposite spin channels. (h) Parabolic fitting within 100 meV below  $E_F$  to the experimental data marked with filled symbols in panels (a–d). Color code is defined in panel (e). The hybridization of these Co QW states with surface-projected W bulk bands [see gray shaded areas in Figs. 5(b) and 5(c)] enhances their magnetization-dependent band asymmetry.

the Co/W system, however, Co films on Mo(110) do not show left-right band dispersion asymmetries, indicating that their origin is related to the spin-orbit effects of the W substrate.

We examine in more detail the link between magnetization and electronic structure of the Co films on W(110) by photoemission measurements with circularly polarized light (the experimental procedure is described in the Supplemental Material [24]). Figures 4(a)–4(d) report second derivative photoemission spectra acquired along  $k_y = 0$  of a 14-ML Co film, for four combinations of light polarization ( $\sigma^+$ ,  $\sigma^-$ ) and sample magnetization ( $\mathbf{M}^\uparrow$ ,  $\mathbf{M}^\downarrow$ ). As a consequence of the dichroic experimental geometry, switching of the light polarization results in a sizeable intensity change of the QW states, that leaves their band dispersion unaltered [34]. This effect can be easily evaluated in Fig. 4(e), that shows momentum distribution curves extracted from Figs. 4(a)–4(d). Red and

orange curves, corresponding to the experimental parameters ( $\sigma^+$ ,  $\mathbf{M}^\uparrow$ ) and ( $\sigma^-$ ,  $\mathbf{M}^\uparrow$ ), display the same sequence of features with opposite intensity ratios at positive and negative  $k_x$  values. Blue ( $\sigma^+$ ,  $\mathbf{M}^\downarrow$ ) and green ( $\sigma^-$ ,  $\mathbf{M}^\downarrow$ ) curves behave similarly.

The magnetization reversal, instead, produces modifications of the QW band dispersion. For example, the features observed along the red and blue curves for  $-0.3 \text{ \AA}^{-1} < k_x < -0.1 \text{ \AA}^{-1}$  appear to be slightly offset ( $0.015 \text{ \AA}^{-1}$ ). More evidently, the two curves present an antiphase behavior for  $-0.85 \text{ \AA}^{-1} < k_x < -0.55 \text{ \AA}^{-1}$ , with the highest positive peak of the red curve ( $k_x = -0.69 \text{ \AA}^{-1}$ ) separated by  $\sim 0.05 \text{ \AA}^{-1}$  from the corresponding peak of the blue curve. Analogous observations can be made for the yellow and green curves at positive  $k_x$  values. These effects turn out to be a manifestation of the left-right asymmetries, already identified in the same energy-momentum space region for the 10-ML Co film

[Fig. 3(b)]. Interestingly, a full reversal of the photoemission band pattern with respect to  $k_x = 0$  is obtained upon switching both magnetization and light polarization. This relation is also valid for all  $k_y = \text{const.}$  lines [24].

In order to describe the magnetization-dependent band asymmetries, we consider a Rashba-type model [35] of a two-dimensional electron gas with an additional exchange interaction (parameter  $I$ ). We assume that the exchange interaction is large enough to pin all electron spins along the magnetization direction. We introduce a Rashba-exchange constant  $\alpha_{\text{RE}}$ , that plays in ferromagnetic systems a similar role as the usual Rashba constant in paramagnetic systems. In general,  $\alpha_{\text{RE}}$  can vary for different QW bands (identified by the main quantum number  $n$ ) and for the opposite exchange-split spin channels [36], as schematically shown in Figs. 4(f) and 4(g). Its size is mainly determined by the potential near the nuclei [37] and its sign depends on the shape of the wave function in that potential gradient [38,39]. The eigenvalues of the system are given by [40,41]

$$E(\mathbf{k}) = \frac{\hbar^2 k_{\parallel}^2}{2m^*} + IM \pm \alpha_{\text{RE}} (\mathbf{k} \times \mathbf{e}_z) \cdot \hat{\mathbf{M}},$$

where  $m^*$  denotes the effective mass and  $\mathbf{e}_z$  an electric field oriented along  $z$ . The Rashba-type term only contributes when  $\mathbf{k}$  is perpendicular to the direction of  $\mathbf{M}$ . We use this model to fit the band dispersion of the QW state displaying the largest magnetization-dependent asymmetry in Figs. 4(a)–4(d) (full black dots). The best parabolic fitting to the experimental data [Fig. 4(h)] gives  $\alpha_{\text{RE}} \sim (2.7 \pm 0.3) \times 10^{-12}$  eV, which is of the same order of magnitude as the Rashba constant obtained in paramagnetic Al films on W(110) [21]. This splitting is much smaller than that of surface features (e.g., in Au(111) [12]) due to the reduced influence of the interface-localized Rashba field on QW states extending over the whole film thickness.

To unveil the nature of the bands observed in the photoemission experiments, we performed DFT calculations for free-standing and W-supported Co films. Figure 5(a) displays the electronic structure of a free-standing 10-ML Co(0001) film (with Co bulk lattice constant). For  $|k_{\parallel}| < 1.0 \text{ \AA}^{-1}$  and energies between 0.5 eV and  $E_F$  we find strongly dispersive spin-up  $sp$  states (red dashed lines) and spin-down  $d$  states (full blue lines). Along the  $\bar{\Gamma} - \bar{K}$  direction some  $d$ -like QW states are predominantly of  $d_{x^2-y^2}$  type, some—with slightly smaller

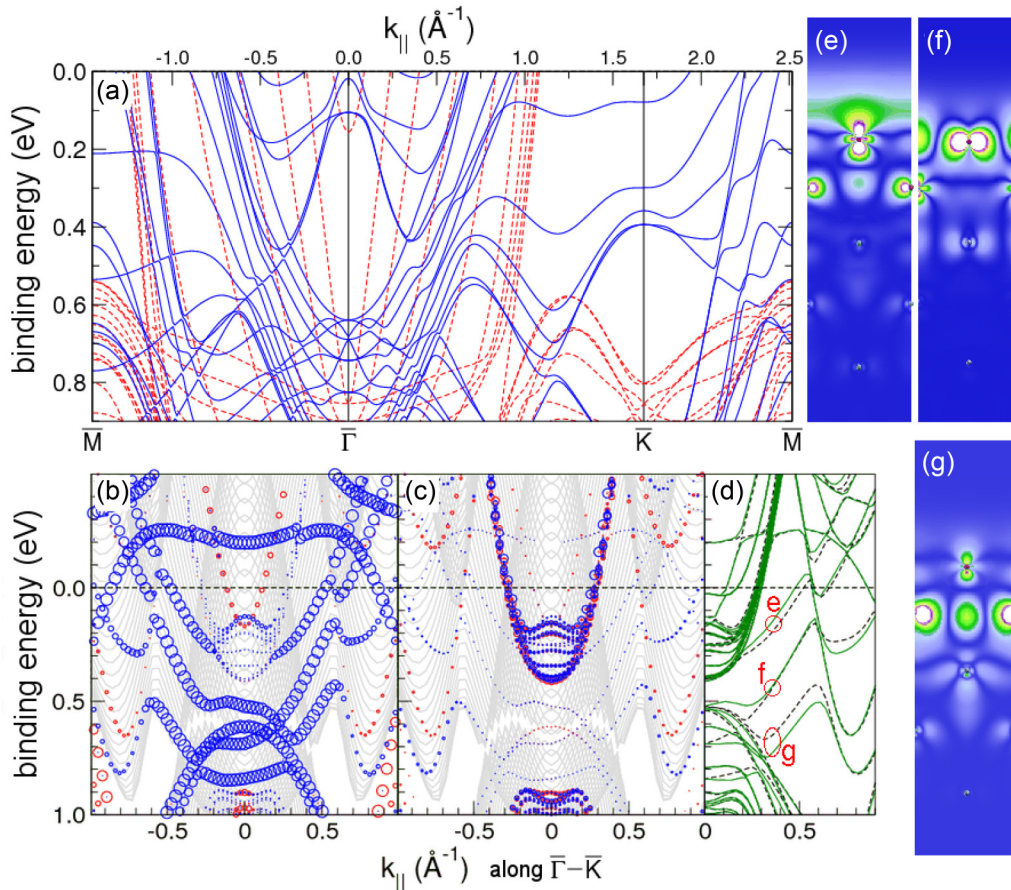


FIG. 5. (Color online) (a) Band structure of a free-standing 10-ML Co(0001) film without spin-orbit coupling (SOC) included in the calculation: red dashed and blue full lines are spin-up and spin-down bands. (b–d) Band structure of two Co layers on W(110) along the [001] axis (corresponding to the  $\bar{\Gamma} - \bar{K}$  or  $k_x$  direction in Co) with SOC included. The size of the symbols indicates the projected weight on the Co layers (b) or at the W side of the interface (c). Color code is the same as defined in panel (a). Gray lines in the background represent the band structure of a thick W(110) layer with SOC included. Panel (d) reports a superposition of the bands displayed in panel (b) for positive (black dashed lines) and negative (green full lines)  $k_{\parallel}$  values. (e–g) Charge-density plots of the states labeled e–g in panel (d), taken in a  $(1\bar{1}00)$  plane that cuts the atomic positions.

dispersion—are more of  $d_z^2$  type. These calculations allow to determine spin and orbital characters of the experimentally observed bands [42–44]. The bands located in the vicinity of  $\bar{\Gamma}$  and displaying oval constant energy contours [Fig. 3(a)] are spin-up  $sp$ -like QW states. Instead, bands showing large magnetization-dependent asymmetries are identified as spin-down  $d$ -like QW states.

The formation of a junction between a Co film and a W(110) crystal determines the interaction among the electronic states of the two materials. More specifically, the extent to which spin-down Co QW states can couple to the underlying substrate depends on three factors: the orbital character (in-plane oriented  $d_{x^2-y^2}$  states will be less sensitive to the interface than out-of-plane oriented  $d_z^2$  states), the main quantum number (e.g., the  $n = 1$  state has a maximum at the center of the magnetic film [Fig. 1(a)], therefore smaller weight at the surface and interface than states with higher  $n$ ), and the energetic position with respect to the (110)-projected W bulk bands (states within a projected gap cannot couple to the substrate).

We analyze the effects of these factors for a simple system, consisting of two Co layers on nine layers of W. In this case the Co film structure is assumed to match the in-plane lattice parameters of W(110) and relax along the out-of-plane direction [45]. The Co magnetization axis is set parallel to the W  $[1\bar{1}0]$  direction [Fig. 2(a)], as in the experiment. As seen in Figs. 5(b)–5(d), the electronic structure perpendicular to the magnetization direction (corresponding to  $\bar{\Gamma} - \bar{K}$  of free-standing Co [Fig. 5(a)]) is highly asymmetric for the spin-down Co bands, i.e.,  $E(k_{\parallel}) \neq E(-k_{\parallel})$ . In Fig. 5(d) the positive and negative  $k_{\parallel}$  directions of Fig. 5(b) are directly compared to emphasize this effect. In detail, we find three Co QW states showing very different dependence on the sign of  $k_{\parallel}$  (or the direction of the magnetization). The state labeled with  $f$  is rather insensitive [ $E(k_{\parallel}) \approx E(-k_{\parallel})$ ],

while the other two,  $e$  and  $g$ , are more strongly influenced by the magnetization direction. These states display energy and momentum separations of [ $\Delta E(e) = -50$  meV,  $\Delta k_{\parallel}(e) = 0.046 \text{ \AA}^{-1}$ ] and [ $\Delta E(g) = 76$  meV,  $\Delta k_{\parallel}(g) = 0.066 \text{ \AA}^{-1}$ ], resulting in  $\alpha_{\text{RE}}(e) = 6.6 \times 10^{-12}$  eV m and  $\alpha_{\text{RE}}(g) = 7.9 \times 10^{-12}$  eV m. Particularly striking is the fact that  $e$  and  $g$  change oppositely with the magnetization direction. Figures 5(e)–5(g) display the charge-density plots of the states labeled  $e$ – $g$ , respectively.  $f$  is dominated by a  $d_{x^2-y^2}$  orbital at the Co surface with a small  $d_z^2$  component at the interface with Co.  $e$  and  $g$  have  $d_z^2$  character at the surface and  $d_{x^2-y^2}$  at the interface. While the former is more surface localized, the latter has more weight at the interface. It is therefore reasonable that a state, which is directed more towards the surface, like  $e$ , has an opposite sign of  $\Delta E$  compared to an interface-oriented state like  $g$ . Moreover,  $|\Delta E|$  and  $\alpha_{\text{RE}}$  are larger for state  $g$ , as they are also influenced by the proximity of the heavy W substrate, where some asymmetric charge distribution is located. This picture is confirmed by calculations where the SOI is not included in W, just in Co: The splitting of  $e$  and  $f$  is unchanged, the one of  $g$  gets smaller. The proximity-induced SOI at the interface becomes larger in energy-momentum regions where the W density of states is higher and for QW states which delocalize more into the substrate. In thicker Co films only some states will show this strong dependence on the magnetization direction, like  $e$  and  $g$ , while most states that are localized in the film, like  $f$ , show only a weak shift with a reversal of  $\mathbf{M}$ .

For a more direct comparison with the experimentally observed bands, we calculate the electronic states of 6 Co ML (with hcp (0001) structure and Co bulk lattice constant) matched with a nine-layers W substrate (Fig. 6). Thicker Co films were also considered and found to display similar behavior. However, a reduced Co film thickness, i.e., a smaller number of Co QW states, permits a clearer visualization of

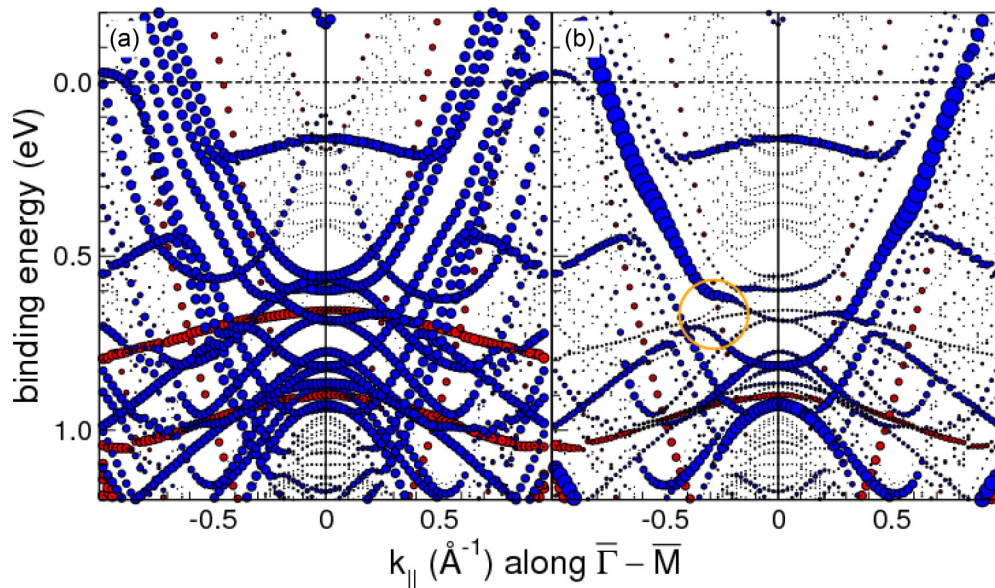


FIG. 6. (Color online) (a) DFT calculations for a 6-ML Co(0001) film on nine layers of W along the  $\bar{\Gamma} - \bar{M}$  direction. The magnetization is set along the Co  $[11\bar{2}0]$  axis. Blue and red dots represent spin-down and spin-up states, respectively. (b) The size of the dots indicates the projected weight at the Co/W interface. The orange circle encloses a gap that opens only for negative  $k_{\parallel}$  values.

the magnetization-dependent band asymmetries near  $E_F$ . The artificial matching of bcc W(110) to hcp Co(0001) corresponds to a compression of about 20% along the W [001] direction [32]. Such a large modification of the W crystal structure may lead to unphysical results in the DFT calculations. In order to avoid such artifacts, we analyze the electronic states of the Co/W junction along the  $\bar{\Gamma} - \bar{M}$  direction [see Fig. 2(a)], where the compression of W (along the [110] axis) is about 2%. Therefore, we set the magnetization along the Co [11 $\bar{2}$ 0] axis, i.e., perpendicular to the experimentally determined easy magnetization axis. As shown in Fig. 6(a), the left-right band asymmetries are clearly visible in the spin-down  $d$ -derived QW states (blue dots) dispersing upward from the  $k_{\parallel} = 0$  and crossing  $E_F$  for  $0.5 \text{ \AA}^{-1} < |k_{\parallel}| < 0.8 \text{ \AA}^{-1}$ . The effects are particularly strong for the interface-localized band, highlighted by large symbols in Fig. 6(b), thus confirming the strength of proximity-induced SOI at the interface. The upward shift of the interface-localized band at negative  $k_{\parallel}$  values is induced by a gap opening (orange circle), that is not at all observed at positive  $k_{\parallel}$  values. The Rashba parameter derived from this shift amounts to  $3.6 \times 10^{-12} \text{ eV m}$ , which compares reasonably well with the value determined experimentally in Fig. 4, despite differences in film thickness and structural parameters. On the basis of this analysis, we conclude that the Co QW states, displaying the largest band asymmetries in the photoemission signal, have an interface-localized spatial character.

Experimental and theoretical results show that the band dispersion is strongly asymmetric along equivalent crystallographic axes and depends on the angle between electron momentum and magnetization direction. These effects are ascribed to exchange and Rashba fields that combine at the buried interface. An important aspect of the present research is the connection with current-induced magnetization switching observed in FM/HM heterostructures. The interface Rashba effect has been assumed to play a central role in

this phenomenon, but has never been directly confirmed experimentally, so far. Our findings demonstrate that Rashba fields indeed are significantly large at atomically flat interfaces and have profound influence on the electronic structure of the magnetic system.

#### IV. CONCLUSIONS

In summary, the observation of QW states in Co films on W(110) provides access to the interface electronic properties of the system and allows a comparison with *ab initio* calculations. The experimental and theoretical analyses concordantly identify unusual features in the ground-state electronic structure of Co films on W(110). Magnetic QW states are found to display an asymmetric band dispersion along equivalent crystallographic directions, which reverses upon switching the film magnetization. This behavior is understood as a combined effect of time reversal and inversion symmetry breaking by the strong exchange and Rashba fields, specific to the Co/W system. The presence of large interface Rashba fields, so far postulated in FM/HM bilayers, has been directly assessed. In perspective, these findings can have broad impact on the understanding of interface effects of fundamental and practical relevance occurring in FM/HM heterostructures.

#### ACKNOWLEDGMENTS

We acknowledge the ‘‘Progetto Premiale, Materiali e dispositivi magnetici e superconduttivi per sensoristica e ICT’’ of the Italian Ministry of Education, University and Research (MIUR), Italy. G.B. is grateful for computing time on the JUROPA supercomputer at the Jülich Supercomputing Centre (JSC), Germany. Financial support from the Deutsche Forschungsgemeinschaft (Grant No. SPP 1666) and the Impuls-und Vernetzungsfonds der Helmholtz-Gemeinschaft (Grant No. HRJRG-408) is gratefully acknowledged.

- 
- [1] I. M. Miron, K. Garello, G. Gaudin, P.-J. Zermatten, M. V. Costache, S. Auffret, S. Bandiera, B. Rodmacq, A. Schuhl, and P. Gambardella, Perpendicular switching of a single ferromagnetic layer induced by in-plane current injection, *Nature* **476**, 189 (2011).
  - [2] L. Liu, O. J. Lee, T. J. Gudmundsen, D. C. Ralph, and R. A. Buhrman, Current-induced switching of perpendicularly magnetized magnetic layers using spin torque from the spin Hall effect, *Phys. Rev. Lett.* **109**, 096602 (2012).
  - [3] P. M. Haney, H.-W. Lee, K.-J. Lee, A. Manchon, and M. D. Stiles, Current-induced torques and interfacial spin-orbit coupling, *Phys. Rev. B* **88**, 214417 (2013).
  - [4] K. Garello, I. M. Miron, C. O. Avci, F. Freimuth, Y. Mokrousov, S. Blügel, S. Auffret, O. Boulle, G. Gaudin, and P. Gambardella, Symmetry and magnitude of spin-orbit torques in ferromagnetic heterostructures, *Nat. Nanotechnol.* **8**, 587 (2013).
  - [5] J. Kim, J. Sinha, M. Hayashi, M. Yamanouchi, S. Fukami, T. Suzuki, S. Mitani, and H. Ohno, Layer thickness dependence of the current-induced effective field vector in Ta|CoFeB|MgO, *Nat. Mater.* **12**, 240 (2013).
  - [6] K. Ando, S. Takahashi, K. Harii, K. Sasage, J. Ieda, S. Maekawa, and E. Saitoh, Electric manipulation of spin relaxation using the spin Hall effect, *Phys. Rev. Lett.* **101**, 036601 (2008).
  - [7] H.-A. Engel, E. I. Rashba, and B. I. Halperin, Out-of-plane spin polarization from in-plane electric and magnetic fields, *Phys. Rev. Lett.* **98**, 036602 (2007).
  - [8] I. Mihai Miron, G. Gaudin, S. Auffret, B. Rodmacq, A. Schuhl, S. Pizzini, J. Vogel, and P. Gambardella, Current-driven spin torque induced by the Rashba effect in a ferromagnetic metal layer, *Nat. Mater.* **9**, 230 (2010).
  - [9] J. C. R. Sánchez, L. Vila, G. Desfonds, S. Gambarelli, J. P. Attané, J. M. De Teresa, C. Magén, and A. Fert, Spin-to-charge conversion using Rashba coupling at the interface between non-magnetic materials, *Nat. Commun.* **4**, 2944 (2013).
  - [10] M. K. Brinkley, Y. Liu, N. J. Speer, T. Miller, and T.-C. Chiang, Using electronic coherence to probe a deeply embedded quantum well in bimetallic Pb/Ag films on Si(111), *Phys. Rev. Lett.* **103**, 246801 (2009).
  - [11] P. Moras, D. Wortmann, G. Bihlmayer, L. Ferrari, G. Alejandro, P. H. Zhou, D. Topwal, P. M. Sheverdyaeva, S. Blügel, and

- C. Carbone, Probing the electronic transmission across a buried metal/metal interface, *Phys. Rev. B* **82**, 155427 (2010).
- [12] S. LaShell, B. A. McDougall, and E. Jensen, Spin splitting of an Au(111) surface state band observed with angle resolved photoelectron spectroscopy, *Phys. Rev. Lett.* **77**, 3419 (1996).
- [13] C. R. Ast, J. Henk, A. Ernst, L. Moreschini, M. C. Falub, D. Pacilé, P. Bruno, K. Kern, and M. Grioni, Giant spin splitting through surface alloying, *Phys. Rev. Lett.* **98**, 186807 (2007).
- [14] I. Barke, F. Zheng, T. K. Rügheimer, and F. J. Himpsel, Experimental evidence for spin-split bands in a one-dimensional chain structure, *Phys. Rev. Lett.* **97**, 226405 (2006).
- [15] M. Hochstrasser, J. G. Tobin, E. Rotenberg, and S. D. Kevan, Spin-resolved photoemission of surface states of W(110)-(1 × 1)H, *Phys. Rev. Lett.* **89**, 216802 (2002).
- [16] M. Z. Hasan and C. L. Kane, Colloquium: Topological insulators, *Rev. Mod. Phys.* **82**, 3045 (2010).
- [17] O. Krupin, G. Bihlmayer, K. Starke, S. Gorovikov, J. E. Prieto, K. Döbrich, S. Blügel, and G. Kaindl, Rashba effect at magnetic metal surfaces, *Phys. Rev. B* **71**, 201403(R) (2005).
- [18] O. Krupin, G. Bihlmayer, K. M. Döbrich, J. E. Prieto, K. Starke, S. Gorovikov, S. Blügel, S. Kevan, and G. Kaindl, Rashba effect at the surfaces of rare-earth metals and their monoxides, *New J. Phys.* **11**, 013035 (2009).
- [19] A. M. Shikin, A. A. Rybkina, A. S. Korshunov, Yu. B. Kudasov, N. V. Frolova, A. G. Rybkin, D. Marchenko, J. Sánchez-Barriga, A. Varykhalov, and O. Rader, Induced Rashba splitting of electronic states in monolayers of Au, Cu on a W(110) substrate, *New J. Phys.* **15**, 095005 (2013).
- [20] A. M. Shikin, A. Varykhalov, G. V. Prudnikova, D. Usachov, V. K. Adamchuk, Y. Yamada, J. D. Riley, and O. Rader, Origin of Spin-Orbit Splitting for Monolayers of Au and Ag on W(110) and Mo(110), *Phys. Rev. Lett.* **100**, 057601 (2008).
- [21] A. G. Rybkin, A. M. Shikin, D. Marchenko, A. Varykhalov, and O. Rader, Spin-dependent avoided-crossing effect on quantum-well states in Al/W(110), *Phys. Rev. B* **85**, 045425 (2012).
- [22] A. Varykhalov, J. Sánchez-Barriga, A. M. Shikin, W. Gudat, W. Eberhardt, and O. Rader, Quantum cavity for spin due to spin-orbit interaction at a metal boundary, *Phys. Rev. Lett.* **101**, 256601 (2008).
- [23] H. Fritzsche, J. Kohlhepp, and U. Gradmann, Epitaxial strain and magnetic anisotropy in ultrathin Co films on W(110), *Phys. Rev. B* **51**, 15933 (1995).
- [24] See Supplemental Material at <http://link.aps.org/supplemental/10.1103/PhysRevB.91.195410> for the experimental geometries used for the photoemission analysis and complementary information on the electronic and magnetic structure of Co films on W(110) and Mo(110).
- [25] H. Krakauer, M. Posternak, and A. J. Freeman, Linearized augmented plane-wave method for the electronic band structure of thin films, *Phys. Rev. B* **19**, 1706 (1979).
- [26] For program description see <http://www.flapw.de>.
- [27] J. P. Perdew, K. Burke, and M. Ernzerhof, Generalized gradient approximation made simple, *Phys. Rev. Lett.* **77**, 3865 (1996).
- [28] C. Li, A. J. Freeman, H. J. F. Jansen, and C. L. Fu, Magnetic anisotropy in low-dimensional ferromagnetic systems: Fe monolayers on Ag(001), Au(001), and Pd(001) substrates, *Phys. Rev. B* **42**, 5433 (1990).
- [29] D. Venus, Interrelation of magnetic-dichroism effects seen in the angular distribution of photoelectrons from surfaces, *Phys. Rev. B* **49**, 8821 (1994).
- [30] J. Bansmann, Surface magnetism of iron and cobalt on W(110) probed with polarized synchrotron radiation, *Appl. Phys. A* **72**, 447 (2001).
- [31] J. Bansmann, L. Lu, M. Getzlaff, M. Fluchtmann, J. Braun, and K. H. Meiwes-Broer, Magnetic linear dichroism in valence band photoemission—a novel technique to study electronic and magnetic properties, *J. Magn. Magn. Mater.* **185**, 94 (1998).
- [32] J. Prokop, D. A. Valdaitsev, A. Kukunin, M. Pratzner, G. Schönhense, and H. J. Elmers, Strain-induced magnetic anisotropies in Co films on Mo(110), *Phys. Rev. B* **70**, 184423 (2004).
- [33] J. S. Park, A. Quesada, Y. Meng, J. Li, E. Jin, H. Son, A. Tan, J. Wu, C. Hwang, H. W. Zhao, A. K. Schmid, and Z. Q. Qiu, Determination of Spin-polarized quantum well states and spin-split energy dispersions of Co ultrathin films grown on Mo(110), *Phys. Rev. B* **83**, 113405 (2011).
- [34] W. Kuch and C. M. Schneider, Magnetic dichroism in valence band photoemission, *Rep. Prog. Phys.* **64**, 147 (2001).
- [35] Yu. A. Bychkov and E. I. Rashba, Properties of a 2D electron gas with lifted spectral degeneracy, *JETP Lett.* **39**, 78 (1984).
- [36] J.-H. Park, C. H. Kim, H.-W. Lee, and J. H. Han, Orbital chirality and Rashba interaction in magnetic bands, *Phys. Rev. B* **87**, 041301 (2013).
- [37] G. Bihlmayer, Yu. M. Koroteev, P. M. Echenique, E. V. Chulkov, and S. Blügel, The Rashba-effect at metallic surfaces, *Surf. Sci.* **600**, 3888 (2006).
- [38] M. Nagano, A. Kodama, T. Shishidou, and T. Oguchi, A first-principles study on the rashba effect in surface systems, *J. Phys.: Condens. Matter* **21**, 064239 (2009).
- [39] H. Bentmann, T. Kuzumaki, G. Bihlmayer, S. Blügel, E. V. Chulkov, F. Reinert, and K. Sakamoto, Spin orientation and sign of the Rashba splitting in Bi/Cu(111), *Phys. Rev. B* **84**, 115426 (2011).
- [40] M. Heide, G. Bihlmayer, Ph. Mavropoulos, A. Bringer, and S. Blügel, Spin-orbit driven physics at surfaces, *Psi-k News. Highlights* **78**, 111 (2006).
- [41] P. Gambardella and I. M. Miron, Current-induced spin-orbit torques, *Philos. Trans. R. Soc., A* **369**, 3175 (2011).
- [42] The energy shift between theory and experiment is due to the different boundary conditions (free-standing vs W-supported Co film) of the two cases and is also observed when we compare calculations for free-standing Co(0001) and Co films on W(110). It originates from the charge transfer occurring from the Co layer to the W substrate, as can be seen, e.g., by a lowering of the work function (by about 600 meV). Experimentally, such effects have already been detected, e.g., for Ni/W(110) [43,44].
- [43] J. Kołaczkiwicz and E. Bauer, The adsorption of Ni on W (110) and (211) surfaces, *Surf. Sci.* **144**, 495 (1984).
- [44] R. A. Campbell, J. A. Rodriguez, and D. Wayne Goodman, The interaction of ultrathin films of Ni and Pd with W(110): An XPS study, *Surf. Sci.* **240**, 71 (1990).
- [45] This choice is determined by the fact that if W is set to the Co in-plane lattice constant, the surface-projected bands of stretched W do not overlap with some of the spin-down Co QW states.